JOURNAL OF AIRCRAFT
Vol. 35, No. 4, July–August 1998

Aeroelastic Response of a Rigid Wing Supported by Nonlinear Springs

Todd O'Neil* and Thomas W. Strganac†
Texas A&M University, College Station, Texas 77843-3141

Nonlinear aeroelastic behavior is examined. This research extends the efforts of several recent investigations that address freeplay or piecewise nonlinearities in aeroelastic systems; however, in the studies described herein the authors address continuous nonlinearities such as those found in structural systems that exhibit spring hardening or softening effects. The authors describe a unique flutter test apparatus designed to permit experimental investigations of prescribed nonlinear response. The results of complementary analytical and experimental studies are presented for a nonlinear aeroelastic system limited to two degrees of freedom.

Nomenclature

a = nondimensional distance (based on semichord) from the midchord to the elastic axis
b = semichord of the wing
C_y = viscous damping coefficient for plunge degree of freedom
C_α = viscous damping coefficient for pitch degree of freedom
f_y = frequency associated with the plunge degree of freedom
f_α = frequency associated with the pitch degree of freedom
g = acceleration caused by gravity
I_e = mass moment of inertia of the wing about the elastic axis
K_y = spring constant for plunge degree of freedom
K_α = spring constant for pitch degree of freedom
k = reduced frequency, $b\omega/V_\infty$
m_T = total mass of test apparatus permitted to plunge
m_w = total mass of test apparatus permitted to pitch
r = distance between the elastic axis and the c.m.
r_b = reference length for Coulomb damping in pitch degree of freedom
T = kinetic energy
V_∞ = freestream velocity
y = coordinate for plunge degree of freedom
α = coordinate for pitch degree of freedom
ζ = nonlinear stiffness parameter for pitch degree of freedom
θ = static angle of attack
μ_y = Coulomb damping coefficient for plunge degree of freedom
μ_α = Coulomb damping coefficient for pitch degree of freedom
ξ = nonlinear stiffness parameter for plunge degree of freedom
ρ = density of air

Presented as AIAA Paper 95-1404 at the AIAA/ASME/ASCE/AHS/ASC 36th Structures, Structural Dynamics, and Materials Conference, New Orleans, LA, April 10–12, 1995; received April 19, 1995; revision received Oct. 30, 1997; accepted for publication March 9, 1998.

*Graduate Research Assistant, Department of Aerospace Engineering. Member AIAA.
†Associate Professor, Department of Aerospace Engineering. Associate Fellow AIAA.

Introduction

AEROELASTICITY is the phenomena resulting from the interaction of structural, inertial, and aerodynamic forces. Although conventional methods of examining aeroelastic behavior rely on a linear approximation of governing equations of the flowfield and structure, aerospace systems inherently contain structural and aerodynamic nonlinearities.[1,2] These nonlinearities result from unsteady aerodynamic sources, large strain-displacement conditions, or the partial loss of structural or control integrity, and these systems exhibit nonlinear dynamic response characteristics such as limit cycle oscillations (LCOs), internal resonances, and chaotic motion.

Nayfeh and Mook[3] describe the adverse consequences of neglecting nonlinearities in models of dynamical systems. As an illustration of nonlinear dynamics, the response of a two-degree-of-freedom spring-pendulum system is examined. The equations of motion for this system contain nonlinearities that couple the two degrees of freedom; yet, the linear form of the equations suggest independent pendulum and translational motion with independent natural frequencies. Nonlinear theory describes an internal resonance phenomena in which a maximum exchange of energy occurs between the degrees of freedom if the higher modal frequencies are integer multiples of the lower modal frequencies. For the spring-pendulum system, this internal resonance occurs if the pendulum mass, length, and spring are tuned such that an integer multiple relationship is achieved for the natural frequencies. The important characteristic of this phenomena is that excitation of one mode will lead to response in another degree of freedom, a phenomena not predictable with the linear equations of motion.

Similar nonlinear behavior for an aeroelastic system has been observed. Cole[4] detected an unexpected response while performing wind-tunnel experiments conducted to identify aeroelastic stability boundaries. Cole used computational methods based on linear theory and the analysis suggested higher dynamic pressures for aeroelastic flutter than those pressures experimentally measured. In the wind-tunnel model used in Cole's experiment, the natural frequency, i.e., in the absence of a freestream velocity, of the second bending mode was greater than twice the frequency of the first torsional mode. Because the frequencies in aeroelastic systems depend upon aerodynamic pressures, the system frequencies may become tuned as a consequence of the aerodynamic effects. The observed response in these experiments suggests that the inaccurate numerical predictions are attributed to limitations arising from the use of linear equations.

Several investigators analytically examined nonlinear aeroelastic behavior.[5–14] Woolston et al.[5] examined freeplay, hys-

teresis, and cubic stiffness nonlinearities. Their results showed that flutter was dependent upon the initial conditions for the freeplay and hysteresis cases; more specifically, an increase in the initial displacements reduced the flutter velocity. LCOs occurred for cubic hardening stiffness, but the stability boundary was insensitive to initial conditions. Breitbach and co-workers[6–8] showed that although flutter solutions based upon linear theory may be appropriate for flutter clearance, a significant number of cases suffer from poor agreement between analysis and test because of the presence of of structural nonlinearities. Breitbach and co-workers focused their efforts on the understanding of nonlinear responses introduced by hysteresis, freeplay, and spring-tab effects on the control system. They also examined the nonlinear flutter equations in the frequency domain to provide a solution method that may be applied to control systems with multiple concentrated nonlinearities.

Lee and LeBlanc[9] performed analytical investigations of systems with cubic nonlinearities. They examined the effects of varying physical system parameters on the flutter envelope and established trends that relate nonlinear response to variations in the initial conditions and nonlinear parameters. They found that systems with spring hardening effects did not experience aeroelastic flutter, rather, only LCO behavior was found. As the freestream velocity was increased, the amplitude of the LCO increased and less transient time was required to achieve LCO behavior. Also, as the wing-to-air mass ratio was increased, the amplitude of the LCO increased. Lee and Desrochers[10] analyzed freeplay and preload nonlinearities, and showed that LCO behavior appeared in regions of otherwise damped oscillations. Price et al.[11] analyzed chaotic response for systems with continuous nonlinear stiffness, demonstrated that chaos occurred, and characterized these possible transitions. Price et al.[12] investigated freeplay nonlinearities in pitch, and identified LCO regions below the linear flutter speed. They also showed the existence of chaotic motion for cases of structural preload.

Tang and Dowell[13] analyzed the effects of freeplay stiffness nonlinearities in the pitch mode using both linear and nonlinear aerodynamic models. They determined that freeplay nonlinearities introduced flutter boundaries at speeds lower than the linear flutter speed. They found that the amplitude of the LCO depended upon velocity, initial conditions, degree of nonlinearity, and initial pitch angle. They observed chaos when the motion approached either the flutter boundary or the stall flutter boundary. Zhao and Yang[14] predicted chaos for systems with stiffness cubic nonlinearities. They determined that chaos occurred for certain elastic axis positions when the velocity was greater than the linear flutter speed.

Several investigators experimentally examined nonlinear aeroelastic behavior.[15–17] These efforts address the effect of freeplay, deadband, and/or piecewise structural nonlinearities (as illustrated in Fig. 1) in aeroelastic systems. Although a few analytical studies have examined continuous structural nonlinearities, the authors are aware of limited experimental investigations that examine continuous structural nonlinearities. Tang and Dowell[15] compared predictions with measurements for a system with continuous nonlinear stiffness behavior in the pitch mode. LCO behavior was found for quadratic and cubic pitching nonlinearities. These LCOs were dependent upon freestream velocity and nonlinear stiffness parameters. It was shown for the case of continuous nonlinearities that the LCO behavior possessed harmonic components of the dominant flutter frequency. Hauenstein et al.[16] performed experiments of aeroelastic chaotic response. These results indicate transitions from LCOs to chaotic responses for aeroelastic systems, but the experiments were limited to systems with freeplay nonlinearities.

Yang and Zhao[17] performed theoretical and experimental flutter investigations on a wing section for freeplay and piecewise stiffness cases. Experiments with piecewise stiffness nonlinearities showed an increase in LCO amplitude for increased freestream velocity. Experiments with freeplay nonlinearities showed LCOs at freestream velocities less than the linear flutter velocity. The LCO amplitude grew with an increase in freestream velocity until the flutter occurred at the linear flutter velocity. Further investigations showed two LCO amplitudes that depended upon the initial condition at the same freestream velocity. This LCO centered about an offset from the static equilibrium position.

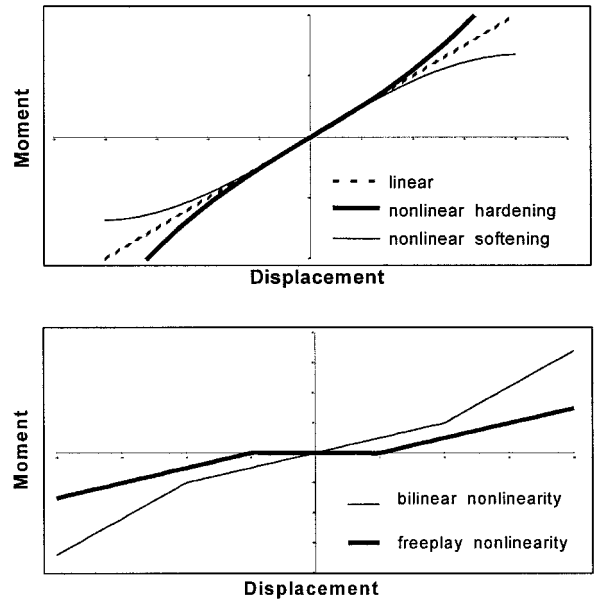

Fig. 1 Nonlinear structural stiffness characteristics are considered in analyses and experiments.

Model

The numerical results consider the aeroelastic response of a wing with cubic nonlinear spring stiffness and with motion limited to two degrees of freedom. For brevity, the equations of motion are presented with minimal development herein; however, the reader is referred to O'Neil[18] for a detailed derivation. As illustrated in Fig. 2, a rigid wing section is mounted to a support system that permits plunge and pitch motion. The displacement and velocity of the c.m., with respect to a coordinate system associated with the elastic axis, are expressed as follows:

$$\boldsymbol{r} = r\cos(\alpha + \theta)\hat{i} + [y + r\sin(\alpha + \theta)]\hat{j} \tag{1}$$

$$\dot{\boldsymbol{r}} = -r\dot{\alpha}\sin(\alpha + \theta)\hat{i} + [\dot{y} + r\dot{\alpha}(\alpha + \theta)]\hat{j} \tag{2}$$

The kinetic energy for the system may be expressed as

$$T = \frac{1}{2}m(\dot{\boldsymbol{r}}\cdot\dot{\boldsymbol{r}}) + \frac{I_{cg}\dot{\alpha}^2}{2} = \frac{m}{2}[\dot{y}^2 + \dot{\alpha}^2 r^2 + 2\dot{y}\dot{\alpha}r\cos(\alpha + \theta)] + \frac{I_{cg}\dot{\alpha}^2}{2} \tag{3}$$

where kinetic energy because of planar rotational motion of the rigid wing is included. Higher-order terms because of kinematic nonlinearities are present in the system, and these components are found from (the kinetic energy terms of) Lagrange's equations[19] as

$$\frac{\partial\left(\dfrac{\partial T}{\partial \dot{y}}\right)}{\partial t} = m[\ddot{y} + \ddot{\alpha}r\cos(\alpha + \theta) - \dot{\alpha}^2 r\sin(\alpha + \theta)] \tag{4}$$

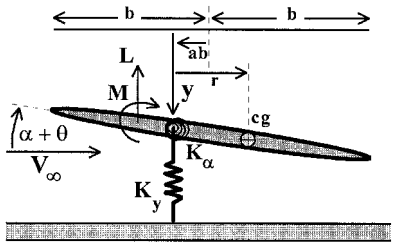

Fig. 2 Aeroelastic system is modeled by a rigid wing section attached to a flexible support that permits pitch and plunge motion.

$$\frac{\partial\left(\frac{\partial T}{\partial \dot{\alpha}}\right)}{\partial t} = m[r\ddot{y}\cos(\alpha+\theta) - ry\dot{\alpha}\sin(\alpha+\theta) + r^2\ddot{\alpha}] + I_{cg}\ddot{\alpha} \tag{5}$$

The equations of motion are derived from these kinetic energy contributions, as well as the potential energy and the work resulting from the internal damping and external aerodynamic forces. The equations of motion are expressed as

$$m_T\ddot{y} + m_w r\cos(\alpha+\theta)\ddot{\alpha} - m_w r\sin(\alpha+\theta)\dot{\alpha}^2 + C_y\dot{y} + \mu_y g m_T(|\dot{y}|/\dot{y}) + K_y(y+\xi y^3) = -L \tag{6}$$

$$m_w r\cos(\alpha+\theta)\ddot{y} + I_e\ddot{\alpha} + C_\alpha + \mu_\alpha m g r_b(|\dot{\alpha}|/\dot{\alpha}) + K_\alpha(\alpha+\zeta\alpha^3) = M \tag{7}$$

where the overdots represent time derivatives, and L and M represent the unsteady aerodynamic lift and moment, respectively. Although θ may be present, it is not used for the studies herein. As will be discussed in the next section, the experiment test apparatus consists of a translating (plunge degree-of-freedom) carriage to which the wing is attached to a rotating (pitch degree-of-freedom) bearing system. Thus, in Eqs. (6) and (7) m_T denotes the total system mass that translates; m_w denotes the wing mass that rotates; and $I_e = r^2 m_w + I_{cg}$, where I_{cg} is the mass moment of inertia of the wing about its c.g.

Both viscous and Coulomb-type damping may be present in the experiments; thus, C_y and C_α terms are included to account for viscous damping forces, and μ_y and μ_α terms are included to account for Coulomb damping forces. Nonlinear stiffness characteristics for pitch and plunge are represented by the parameters ζ and ξ. Higher-order terms, including the centripetal acceleration term $r\dot{\alpha}^2$ and stiffness nonlinearities, as well as the transcendental terms are retained to capture those sources of dynamic coupling. Typically, these terms are assumed negligible and it is noted that the linear form of Eqs. (6) and (7) are identical to the classical pitch and plunge equations found in numerous publications.[20,21]

These equations appear to be uncoupled for the case of $r = 0$; yet, it is important to note that the unsteady aerodynamic loads are dependent upon the motion of the wing, thus,

$$L = L(\dot{y}, \ddot{y}, \alpha, \dot{\alpha}, \ddot{\alpha}, V_\infty, \rho, \text{time}) \tag{8}$$

$$M = M(\dot{y}, \ddot{y}, \alpha, \dot{\alpha}, \ddot{\alpha}, V_\infty, \rho, \text{time}) \tag{9}$$

and, as such, provide an additional source of coupling for the system.

Although the dynamic response because of kinematic and structural nonlinearities is examined, the aerodynamic lift and moment is found to be linear (an assumption validated by the experiments discussed in the subsequent sections) for the range of motion of these studies. Thus, a linear unsteady aerodynamic model is appropriate. The aerodynamic lift and moment are modeled by the unsteady aerodynamic theory of Theodorsen[22]

$$L = \pi\rho b^2(\ddot{y} + V_\infty\dot{\alpha} - ba\ddot{\alpha}) + 2\pi\rho V_\infty Cb(\dot{y} + V_\infty\alpha + b(\tfrac{1}{2} - a)\dot{\alpha}) \tag{10}$$

$$M = -\pi\rho b^3(-a\ddot{y} + (\tfrac{1}{2} - a)V_\infty\dot{\alpha} + (\tfrac{1}{8} - a^2)b\ddot{\alpha}) + 2\pi\rho V_\infty Cb^2(\tfrac{1}{2} + a)(\dot{y} + V_\infty\alpha + b(\tfrac{1}{2} - a)\dot{\alpha}) \tag{11}$$

where C is Theodorsen's function that depends on the reduced frequency, $k = b\omega/V_\infty$. It is noted that Eqs. (10) and (11) represent incompressible, small disturbance unsteady flow.

The approach used to solve the equations of motion is outlined in the Results section.

Experiment

The two-degree-of-freedom analytical model is the basis for the development of the experiment test apparatus. Physical properties of the experiment hardware and associated analyses are provided next: $a = -0.450$; $m_T = 10.3$ kg; $m_w = 1.662$ kg; $b = 0.1064$ m; span $s = 0.6$ m; airfoil profile = NACA 0012; $K_\alpha = 2.57$ N-m/rad (linear case) and $K_\alpha(1 + \zeta\alpha^2) = 2.57\ (1 + 1.33\alpha^2)$ N-m/rad (nonlinear case); $K_y = 2860$ N/m (linear case) and $K_y(1 + \zeta y^2) = 2860\ (1 + 0.09\ y^2)$ N/m (nonlinear case); $r = 0.0287$ m; $C_y = 7.30$ kg/s; $C_\alpha = 0.008$ kg-m^2/s; $\mu_y = 0.0125$ C; $\mu_\alpha = 0.0252$ C; $I_e = 0.0160 + r^2 m_w = 0.0174$ kg-m^2; $Y_0 = 0.0254$ m; $\alpha_0 = 0.175$ rad; and initial conditions in velocity = 0. The test apparatus permits nonlinear pitch and plunge response of a rigid wing section, and the design of the test apparatus permits independent motion in both degrees of freedom. As illustrated in Fig. 3, translational motion associated with the plunge degree of freedom is governed by a carriage mounted on rails. And, as illustrated in Fig. 3, rotational motion associated with the pitch degree of freedom is governed by rotational bearings mounted to this carriage. The pitch and plunge motions are constrained by springs that are selected to examine stiffness effects on dynamic response. Protective constraints limit the excessive amplitude of motion associated with flutter without effecting the onset of flutter, i.e., the constraints are positioned well beyond the range of reasonable pitch and plunge amplitudes.

Nonlinear structural response in the experiments is governed by a pair of cams (see Fig. 3), which are designed to permit tailored linear or nonlinear response. The shape of each cam dictates the nature of the nonlinearity; thus, with this approach, these cams provide a large family of prescribed responses. For the studies herein, the pitch cam is manufactured to provide continuous nonlinear restoring loads that behave as a spring with cubic response, and the plunge cam is manufactured to provide linear restoring loads that behave as a spring with linear response (although measurements indicate a slight nonlinearity is present).

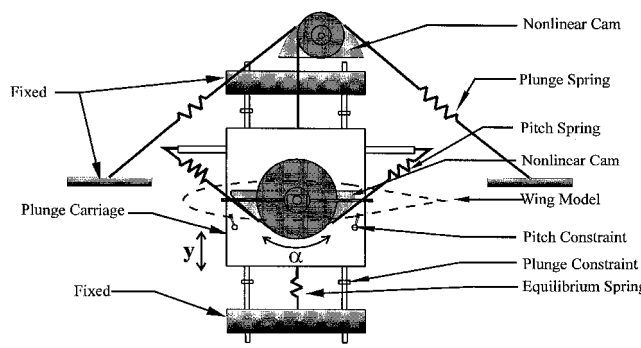

Fig. 3 Flutter apparatus allows motion in two degrees of freedom. Nonlinear pitch and plunge response is introduced through two cams with prescribed nonlinear shapes.

Flutter may be investigated without wing failure; thus, instead of approaching the linear flutter boundary and extrapolating to predict its location, actual linear flutter conditions may be achieved. Physical parameters such as the support stiffness, the mass (and associated mass distribution), the moment of inertia of the wing, the location of the elastic axis, and the airfoil shape, may be easily modified to experimentally determine their effect on the flutter conditions. Because the design of the test apparatus, and its influence on flutter analysis, the total mass of the wing and support structure is considered as this total mass affects the plunge response. However, the mass moment of inertia does not include the contribution of the translational carriage as this component does not pitch.

The current investigations utilize the 2 ft × 3 ft low-speed wind tunnel at Texas A&M University; this facility provides temperature-controlled freestream velocities up to 46 m/s. The test apparatus is attached to the underside of the wind-tunnel test section and, in this configuration, the rigid wing section is mounted vertically and it is the only article exposed to the flowfield. In addition, this mounting position reduces the total frictional forces acting on bearing surfaces of the test apparatus hardware. To measure response, accelerometers are mounted on the rotating pitch cam and the translating carriage, and optical encoders are mounted on rotating shafts of the test apparatus. The test approach is outlined in the following section.

Results

These studies examine nonlinear dynamical pathologies such as LCO and internal resonance responses as discussed in detail in the Introduction. Nonlinear stiffness characteristics that lead to LCO response are considered. Also, of particular motivating interest is the atypical behavior present in the experiments of Cole.[4] Thus, the pitch and plunge modes that might aeroelastically couple are tailored such that the frequencies may shift to the integer relationship necessary for internal resonance behavior at freestream velocities less than the flutter velocity. Predicted responses obtained from the analytical model and measured responses obtained from the experiments are compared. The physical properties of the wing section and experimental apparatus are presented in the previous section.

The equations of motion are integrated following the approach used by Lee and LeBlanc[9] and Lee and Desrochers,[10] wherein the finite difference approximation of Houbolt[23] is used (also see O'Neil[18]) to provide equations for the nonlinear system. The approach is limited to third-order accuracy because of the starting procedure. Jones and Lee[24] examined a single-degree-of-freedom model with a cubic restoring force in the absence of aerodynamic loads, and showed that Houbolt's method compared well to higher-order methods. The response is found using the IMSL[25] nonlinear solution package (DNEQNF) to solve nonlinear equations. The integration time step is 1/256th of the shorter period of two free vibration modes.[9]

Theodorsen's function, $C(k)$, contained within the description of the unsteady aerodynamic loads [see Eqs. (10) and (11)], depends on the reduced frequency k. Similar to the efforts of Price et al.,[12] the impact of the assumptions contained in quasisteady and unsteady aerodynamic models were considered. For the low reduced frequency motion of the experiments discussed herein ($k \approx 0.1$), a quasisteady assumption is proven valid by preliminary experiments and, consequently, $C(k)$ is set to unity for subsequent analyses.

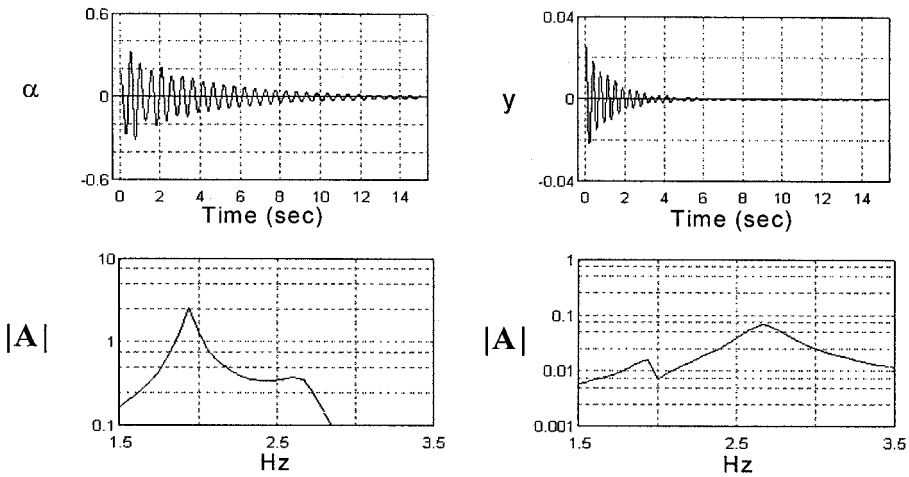

Fig. 4 Predicted free response is shown at V_∞ = 0 m/s for the constant stiffness system.

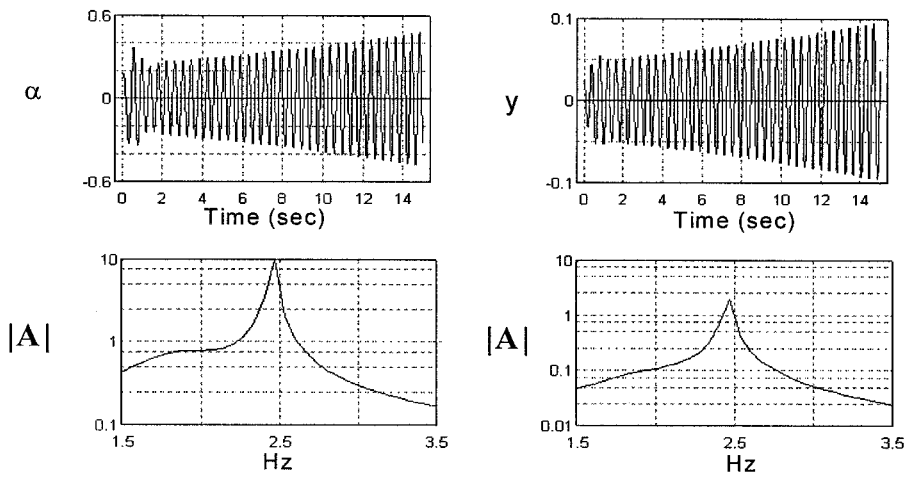

Fig. 5 Predicted aeroelastic response is shown at flutter conditions ($V_\infty \approx$ 15.0 m/s) for the constant stiffness system.

Structure with Constant Stiffness

Figure 4 presents predictions of plunge and pitch response for a zero freestream velocity. The elastic axis is located at 27% of the chord and the c.g. is located at 41% of the chord. Minimum coupling is evident in the plunge motion, whereas there is significant coupling indicated in the pitch response. However, as shown by the fast fourier transforms (FFTs), the frequency of motion associated with coupled pitch ($f_\alpha \approx 1.9$ Hz) and plunge ($f_y \approx 2.7$ Hz) response is evident in both degrees of freedom. Phase-plane portraits (not shown for brevity) verify a stable decaying motion. The response reflects damping from viscous and Coulomb sources as well as aerodynamic damping present from the wing oscillating in air. Figure 5 presents the predicted response for a freestream velocity slightly greater than the flutter velocity ($V_{\infty,\text{flutter}} \approx 15.0$ m/s). Growing motion is evident in the response of both degrees of freedom. As shown by the FFTs, the frequency of motion is identical for both degrees of freedom ($f = f_y \approx 2.5$ Hz). Phase-plane portraits verify an unstable growing motion.

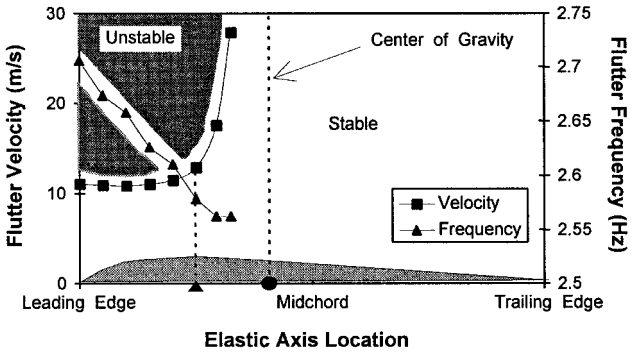

Fig. 6 Measured flutter velocities and associated aeroelastic frequencies are shown for several locations of the elastic axis. Constant stiffness is present.

Experiments are performed to validate these predictions as well as examine the sensitivity of the response to system parameters. Tests are conducted by achieving a target freestream velocity and then releasing the system from a fixed initial displacement in pitch and/or plunge. The response to this initial condition is measured with the accelerometers and the optical encoders. Aeroelastic response, and the onset of any instability, is examined by monitoring the system frequencies and damping characteristics for increasing flow conditions. The content of the accelerometer signals is analyzed using FFT methods. Frequency and damping behavior of the response are found prior to moving to the next test point.

The measured flutter velocity and frequency for several positions of the elastic axis are presented in Fig. 6. In comparison to predicted results, slight differences are noted in both flutter velocity and frequency; these differences are attributed to unmodeled nonlinearities (see Concluding Remarks). These re-

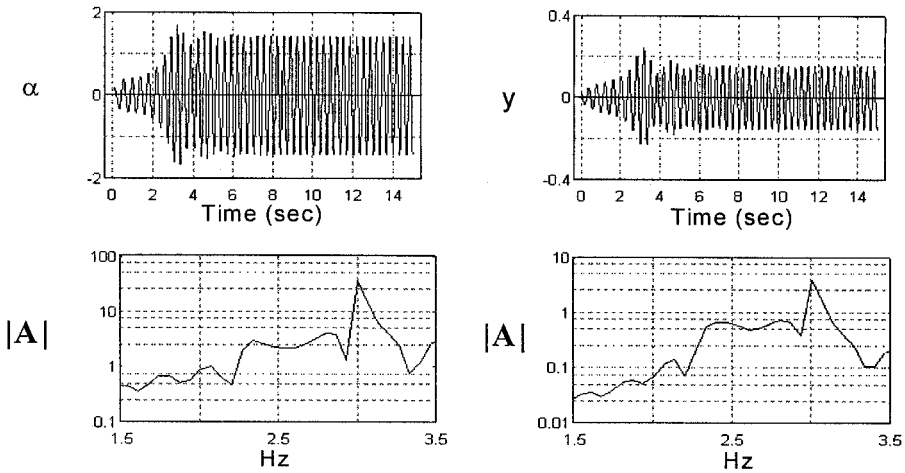

Fig. 7 Predicted aeroelastic response is shown at $V_\infty \approx 15.0$ m/s for the nonlinear system ($\xi = 0.09$ and $\zeta = 1.33$).

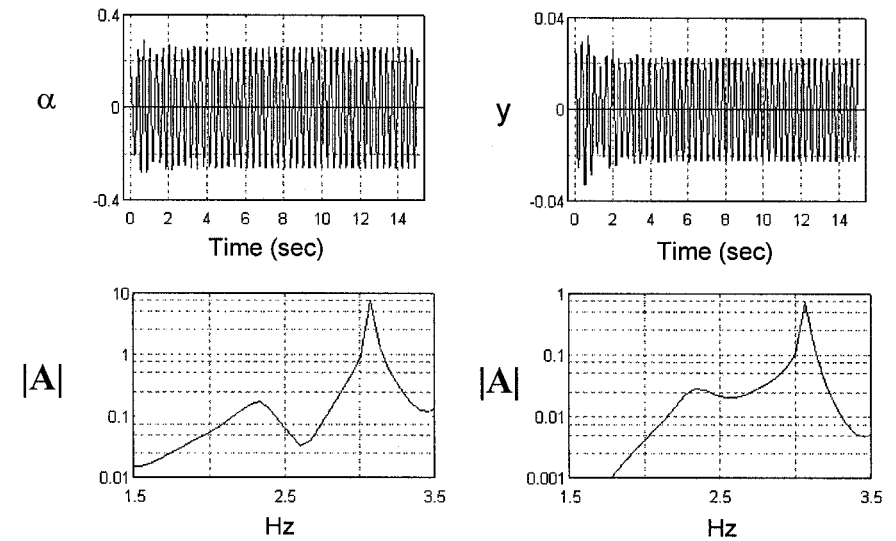

Fig. 8 Predicted aeroelastic response is shown at $V_\infty \approx 15.0$ m/s for the nonlinear system ($\xi = 0.09$ and $\zeta = 50$).

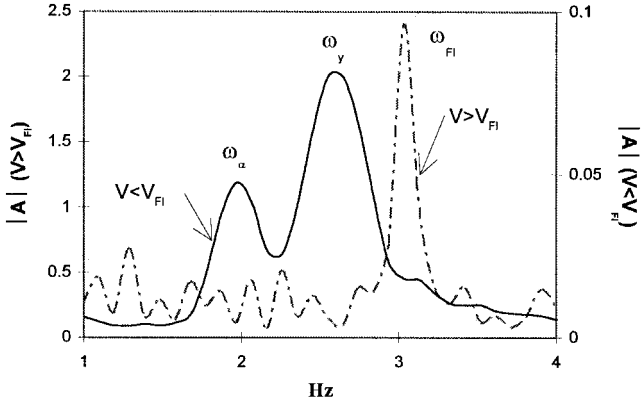

Fig. 9 Frequency responses, derived from experiments performed to validate predictions, are shown for two cases. Two distinct frequencies are observed at a subcritical velocity ($V_\infty \approx 5.0$ m/s) and a single distinct frequency is observed at the flutter velocity ($V_\infty \approx 16.5$ m/s).

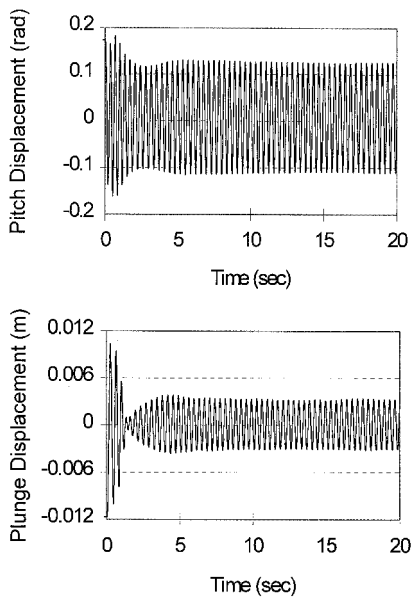

Fig. 10 Measured aeroelastic response is shown at V_∞ 15.2 m/s for the nonlinear system ($\xi = 0.09$ and $\zeta = 500$).

sults show that flutter is suppressed as the elastic axis is toward the center of gravity. This behavior agrees with the design philosophy that flutter may be attenuated with mass balancing of the system.[26]

Structure with Nonlinear Stiffness

In the analyses of nonlinear behavior, springs are tailored to provide specified cubic hardening structural response in both degrees of freedom. Spring constants and nonlinear stiffness coefficients for both degrees of freedom are presented in the Experiment section. The nonlinear coefficients are found by performing a cubic fit to measurements of load vs deformation.

Figure 7 presents the predicted nonlinear plunge and pitch response for a freestream velocity slightly greater than the flutter velocity ($V_{\infty,\text{flutter}} \approx 15.0$ m/s) predicted for the constant stiffness, i.e., linear flutter, case. The response of the test apparatus is subject to nonlinearities in aerodynamics, and the predicted response shows limit cycle oscillations occur with an amplitude that is too large to be compared by experiments ($\alpha >> \alpha_{\text{stall}}$). Although aerodynamic nonlinearities are of interest and will be the subject of future efforts, the nonlinear stiffness characteristic in pitch ($\zeta = 1.33$) is not significant enough

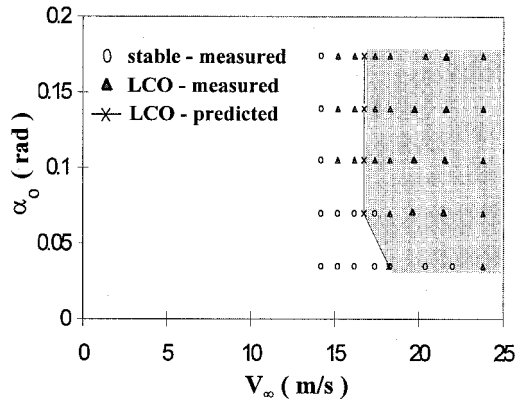

Fig. 11 Map of possible LCO response as affected by freestream velocities and initial conditions is shown. The shaded region indicates the regime of predicted LCO response.

to produce experimentally observable limit cycle oscillations within the linear aerodynamic range. Analysis is performed to determine the pitch nonlinear stiffness coefficient necessary to produce observable limit cycle oscillations by experiment. Figure 8 presents the predicted response using a nonlinear stiffness coefficient of $\zeta = 50$ and a freestream velocity slightly greater than the linear flutter case. The frequency of oscillation associated with the LCO is approximately 3.1 Hz.

Wind-tunnel tests are performed in which the test apparatus has a nonlinear pitch cam and a linear plunge cam. As a consequence of a change in the nonlinear cam used to reduce the amplitude of the LCO, measurements are obtained with the elastic axis repositioned at 30% of the chord (a 3% shift rearward). For this configuration, the measured natural frequencies are 1.96 Hz for the pitch degree of freedom and 2.77 Hz for the plunge degree of freedom. Analysis of this configuration predicts a flutter velocity of 16.5 m/s and a flutter frequency of 2.55 Hz. The cubic stiffness prevents conventional, i.e., unbounded growth, flutter; however, the onset of LCOs occur at a freestream velocity of 16.5 m/s, and this speed is similar to that found by linear analysis. Figure 9 shows the frequency content derived from FFTs of the measured responses. Two cases are shown: First, the frequency of pitch and plunge response at a freestream velocity below the flutter velocity ($V_\infty \approx 5$ m/s); and second, the frequency of the coalesced aeroelastic mode at a freestream velocity of 16.5 m/s. The measured frequency of oscillation associated with the LCO is approximately 3.1 Hz, as also found by analysis.

The affect of the initial conditions and nonlinear stiffness on the aeroelastic response coefficient is of interest. A coefficient of $\zeta = 50$ (as used previously) produces the largest acceptable limit cycle amplitude ($\alpha \approx 14$ deg); and, as one should expect, larger values of ζ will lead to LCOs with smaller amplitudes. Consistent with the findings of Lee and LaBlanc[9] and Tang and Dowell,[15] it is observed that higher freestream velocities lead to LCOs with larger amplitudes, and it is noted that these larger amplitudes may exceed aerodynamic stall conditions and must be considered accordingly. Thus, a 10-fold increase in the nonlinear stiffness coefficient ($\zeta = 500$) is used to limit the amplitude of LCO to the linear aerodynamic range for parametric studies associated with initial conditions.

Figure 10 presents measurements of LCO response for a freestream velocity of 15.2 m/s. The frequency of response is 2.76 Hz. It is noted that the freestream velocity for the onset of the LCO, the amplitude of the LCO, and the frequency of the LCO are reduced from the previous cases because of the increased nonlinearity in stiffness. Experiments are conducted to examine the effect of initial conditions on the onset of LCO response. Figure 11 presents a mapping of the presence of LCO response as affected by freestream velocities and initial conditions. The shaded region indicates the regime in which LCO response is predicted to occur and solid symbols indicate

test points in which LCO response is measured. Good agreement is evident. Unlike the analytical efforts of Woolston[5] and Lee and LaBlanc,[9] these results show a sensitivity to initial conditions that are attributed to the presence (and model) of Coulomb damping.

Concluding Remarks

Aeroelastic behavior is investigated both analytically and experimentally for systems that exhibit nonlinear structural response. Specifically, cubic nonlinear stiffness effects are studied, and these efforts represent a natural extension of recent studies of freeplay and piecewise nonlinearities. A unique test apparatus is developed that permits tailored experimental investigations of nonlinear aeroelastic response.

The equations of motion used in the model retain kinematic nonlinearities, and both viscous and Coulomb damping models are used to represent structural damping evident in the experiments. Prescribed cam shapes and spring stiffnesses are used to introduce specific nonlinear stiffness responses for the aeroelastic system. The impact of the assumptions contained in quasisteady and unsteady aerodynamic models are considered. For the low reduced frequency motion of the experiments discussed herein ($k \approx 0.1$), a quasisteady assumption is proven valid by preliminary experiments and, consequently, Theodorsen's function $C(k)$ is set to unity for subsequent analyses. Obviously, this assumption must be validated as the reduced frequency is increased.

Analytical results are found to be consistent with the findings of others. For instance, these results agree well with the findings of Woolston et al.[5] and Lee and LeBlanc,[9] who indicate transitions from stable to unstable responses, and their associated limit cycle oscillations, for systems with cubic nonlinearities. Regions of oscillations with decaying amplitude, which transition to limit cycle oscillations for increased freestream velocities, are predicted.

The results of experimental studies utilizing the test apparatus show good agreement with supporting analytical studies. Both viscous and Coulomb damping forces, attributed to the design of the test apparatus, are evident in measurements. In particular, the bearing design in the test apparatus leads to friction loads that are best modeled by Coulomb damping. It was suggested that the damping coefficients may be nonlinear for cases with Coulomb damping because significant damping occurs for low velocities and small damping exists for high velocities. Such damping is one of the most significant nonlinearities that is difficult, yet necessary, to model. Differences between measurements and predictions are most likely attributed to unmodelled nonlinearities in damping and should be considered an issue for future study.

Evidence of internal resonance behavior in aeroelastic systems is of interest, but the possible internal resonance behavior that was experimentally observed in previous windtunnel investigations is not replicated herein. The pitch and plunge modes must be tuned such that the aeroelastic frequencies are not integer multiples at zero freestream velocity, but do satisfy this integer relationship at a velocity less than the flutter velocity. For internal resonances to exist for a system coupled by cubic nonlinearities, a 3:1 frequency ratio must be present. Unfortunately, characteristics of the present configuration do not lead to this integer relationship. Future investigations will address these configuration requirements.

Acknowledgment

This research was partially supported under NASA Grant NAG1-1618, the authors wish to thank NASA Langley Research Center for this support.

References

[1]Dowell, E. H. (ed.), Curtiss, H. C., Jr., Scanlan, R. H., and Sisto, F., *A Modern Course in Aeroelasticity*, 2nd ed., Kluwer Academic, Norwell, MA, 1989.

[2]Dowell, E. H., "Nonlinear Aeroelasticity," *Proceedings of the AIAA 31st Structures, Structural Dynamics, and Materials Conference*, AIAA, Washington, DC, 1990, pp. 1497–1509.

[3]Nayfeh, A. H., and Mook, D. T., *Nonlinear Oscillations*, Wiley, New York, 1979.

[4]Cole, S. R., "Effects of Spoiler Surfaces on the Aeroelastic Behavior of a Low-Aspect Ratio Wing," *Proceedings of the AIAA 31st Structures, Structural Dynamics, and Materials Conference*, AIAA, Washington, DC, 1990, pp. 1455–1463.

[5]Woolston, D. S., Runyan, H. L., and Andrews, R. E., "An Investigation of Effects of Certain Types of Structural Nonlinearities on Wing and Control Surface Flutter," *Journal of the Aeronautical Sciences*, Vol. 24, No. 1, 1957, pp. 57–63.

[6]Breitbach, E. J., "Flutter Analysis of an Airplane with Multiple Structural Nonlinearities in the Control System," NASA TP 1620, March 1980.

[7]Breitbach, E., "Effects of Structural Nonlinearities on Aircraft Vibration and Flutter," AGARD-R-665, Jan. 1978.

[8]Breitbach, E. J., "Treatment of the Control Mechanism of Light Airplanes in the Flutter Clearance Process, Science and Technology of Low Speed and Motorless Flight," NASA CP 2085, Pt. II, 1979, pp. 437–466.

[9]Lee, B. H. K., and LeBlanc, P., "Flutter Analysis of a Two-Dimensional Airfoil with Cubic Nonlinear Restoring Force," National Aeronautical Establishment, Aeronautical Note 36, National Research Council (Canada) No. 25438, Ottawa, PQ, Canada, 1986.

[10]Lee, B. H. K., and Desrochers, J., "Flutter Analysis of a Two-Dimensional Airfoil Containing Structural Nonlinearities, National Aeronautical Establishment," Aeronautical Rept. LR-618, National Research Council (Canada) No. 27833, Ottawa, PQ, Canada, 1987.

[11]Price, S. J., Alighanbari, H., and Lee, B. H. K., "The Aeroelastic Response of a Two-Dimensional Airfoil with Bilinear and Cubic Structural Nonlinearities," *Proceedings of the AIAA 35th Structures, Structural Dynamics, and Materials Conference*, AIAA, Washington, DC, 1994, pp. 1771–1780.

[12]Price, S. J., Alighanbari, H., and Lee, B. H. K., "Postinstability Behavior of a Two-Dimensional Airfoil with a Structural Nonlinearity," *Journal of Aircraft*, Vol. 31, No. 6, 1994, pp. 1395–1401.

[13]Tang, D. M., and Dowell, E. H., "Flutter and Stall Response of a Helicopter Blade with Structural Nonlinearity," *Journal of Aircraft*, Vol. 29, No. 5, 1992, pp. 953–960.

[14]Zhao, L. C., and Yang, Z. C., "Chaotic Motions of an Airfoil with Non-Linear Stiffness in Incompressible Flow," *Journal of Sound and Vibration*, Vol. 138, No. 2, 1990, pp. 245–254.

[15]Tang, D. M., and Dowell, E. H., "Comparison of Theory and Experiment for Non-Linear Flutter and Stall Response of a Helicopter Blade," *Journal of Sound and Vibration*, Vol. 165, No. 2, 1993, pp. 251–276.

[16]Hauenstein, J., Laurenson, R. M., Eversman, W., Galecki, G., Qumei, I., and Amos, A. K., Chaotic Response of Aerosurfaces with Structural Nonlinearities, *Proceedings of the AIAA 31st Structures, Structural Dynamics, and Materials Conference*, AIAA, Washington, DC, 1990, pp. 1530–1539.

[17]Yang, Z. C., and Zhao, L. C., "Analysis of Limit Cycle Flutter of an Airfoil in Incompressible Flow," *Journal of Sound and Vibration*, Vol. 23, No. 1, 1988, pp. 1–13.

[18]O'Neil, T., "Experimental and Analytical Investigations of an Aeroelastic Structure with Continuous Nonlinear Stiffness," M.S. Thesis, Texas A&M Univ., College Station, TX, May 1996.

[19]Meirovitch, L., *Methods of Analytical Dynamics*, McGraw–Hill, New York, 1970.

[20]Scanlan, R. H. and Rosenbaum, R., *Introduction to the Study of Aircraft Vibration and Flutter*, MacMillan, New York, 1952.

[21]Fung, Y. C., *An Introduction to the Theory of Aeroelasticity*, Wiley, New York, 1955.

[22]Theodorsen, T., "General Theory of Aerodynamic Instability and the Mechanism of Flutter," NACA Rept. 496, 1935.

[23]Houbolt, J. C., "A Recurrence Matrix Solution for the Dynamic Response of Elastic Aircraft," *Journal of the Aeronautical Sciences*, Vol. 17, No. 9, 1950, pp. 540–550.

[24]Jones, D. J., and Lee, B. H. K., "Time Marching Numerical Solution of the Dynamic Response of Nonlinear Systems, National Aeronautical Establishment," Aeronautical Note 25, National Research Council (Canada), No. 24131, Ottawa, ON, Canada.

[25]*Nonlinear Equations, User's Manual*, Vol. 2, Version 1.1, International Mathematical and Statistical Library, 1989.

[26]Pines, S., "An Elementary Explanation of the Flutter Mechanism," *Proceedings of the National Specialists Meeting on Dynamics and Aeroelasticity*, Inst. of the Aeronautical Sciences, Ft. Worth, TX, 1958, pp. 52–58.